Hindawi
Journal of Nanomaterials
Volume 2022, Article ID 7510499, 8 pages
https://doi.org/10.1155/2022/7510499

Research Article

Analysis and Experimental Investigation of A356 Aluminium Alloy Hybrid Composites Reinforced with Gr-FE_3O_4-B_4C Nanoparticles Synthesised by Selective Laser Melting (SLM)

J. Anoop,[1] Vijay Ananth Suyamburajan,[1] P. Sekhar Babu,[2] and Sisay Addis Filketu[3]

[1]*Department of Mechanical Engineering, Vels Institute of Science, Technology & Advanced Studies (VISTAS), Chennai, Tamilnadu, India*
[2]*Department of Mechanical Engineering, Narsimha Reddy Engineering College, Hyderabad, India*
[3]*School of Mechanical and Industrial Engineering, Institute of Technology, Debre Markos University, Debre Markos, Ethiopia 269*

Correspondence should be addressed to Sisay Addis Filketu; sisayaddis123@gmail.com

Received 27 April 2022; Accepted 22 June 2022; Published 9 July 2022

Academic Editor: V. Vijayan

Additive manufacturing techniques (AMTs) evolved quickly from simple prototype options to promising additive manufacturing techniques. The additive technologies, which include point-by-point material merging, full melting, and solidification of powder particles, provide potential unique braves and advantages with nanometal powders. In the fabrication of A356 aluminium alloy-based hybrid metal matrix nanocomposites, graphite (Gr), iron oxide (Fe_3O_4), and boron carbide (B_4C) are used as nanoreinforcement. Famous AMTs like selective laser melting have created A356 hybrid nanocomposites (SLM). The ingot was made out of a cylindrical slot measuring 14×100 mm. The percentages 2%, 4%, and 6% are added to the reinforcements Gr, Fe_3O_4, and B_4C. Microtensile and microhardness tests were used to determine the outcome of the reinforcement. Microtensile and microhardness parameters are assessed using microtensile test equipment and a Vickers hardness tester, with the specimen prepared in accordance with ASTM standards. A356 with 2, 4, and 6% reinforcing has a Vickers Hardness Number (VHN) of 144, 163, and 188, respectively. As the boron carbide reinforcement is increased, the load value of graphite and iron oxide (2, 4, and 6%) rises. The greatest ultimate tensile strengths are 260.10, 290.06, and 325.43 N/mm^2, respectively. The bonding structure of nanocomposites is assessed using an OM, and then, microtensile specimens are assessed using a SEM. As a result of the superior effect of the diverse reinforcements Gr, Fe_3O_4, and B4C, more increased tensile and hardness qualities have been attained.

1. Introduction

Nowaday's rapid developments in engineering and technology have a huge demand for lightweight and high-strength materials with good tensile, wear, and hardness properties for particular use in aeronautical, automobile, medical, marine, and defence departments. Aluminium and their alloys are espoused in enormous applications, in particular aeronautical, automobile, medical, sports, defence, petrochemical engineering, and marine, outstanding to their superb properties like high strength, good thermal conductivity, high wear, and corrosion resistance [1–3]. Most of the researchers used casting [4, 5], powder metallurgy [6–8], and heat treatment techniques [9–11] to improve the mechanical properties of aluminium alloys. These traditional techniques are inadequate to meet technological demand. The application of modern advancement to the manufacturing of products and parts with high mechanical properties is the major intention of material processing.

Metal matrix composites (MMCs) are an essential role in lightweight and high-strength materials that venture to coalesce the high solidness, stiffness, and sturdiness provided by a metal matrix [12–14]. Research shows that the formation of metal matrix composites with the addition of the different reinforcements into the matrix can improve the mechanical properties appreciably. Generally

used reinforcements include particle, whisker, and fiber. When comparing whisker and fiber, particle reinforcement has more benefits produced in the matrix such as processing, uniform microstructure, and cost [15]. Consequently, particle reinforcement MMCs have been used in aeronautical industries, automotive industries, and medical and defence departments. Nanoparticles by adding a metal matrix improve the strength of MMCs extensively due to disarticulation and dispersal strengthening. Nanoparticles assist to enhance mechanical properties such as strength, wear resistance, and hardness of MMCs [16].

When high strength is required, A356 aluminium casting alloys are employed in the manufacture of aviation components. The need for lightweight, high-strength components is expanding all the time. Aluminium matrix composites are being touted as a new generation of possible materials for a wide range of technical applications. For Aluminium Metal Matrix Composites (AMMCs), generally used nanoparticle reinforcement contains B_4C, SiC, Gr, TiB_2, Al_2O_3, and TiC [17–19].

B_4C is an elegant reinforcement material because of its superb strength, microhardness, wear resistance, high specific stiffness, good damping capacity, excellent thermal conductivity, chemical and thermal stability, high melting point, high wettability, low density, and good interfacial bonding property with aluminium comparable to Al_2O_3, TiB_2, TiC, and SiC [20–22].

Dirisenapu et al. [23] reported that the tensile strength of the nanocomposites increased with an increase in B_4C nanoparticles and percentage of elongation; density is decreased.

Chandrasekaran et al. [24] investigated Al-B_4C cermet fabricated by additive manufacturing; the hardness of the composite reached as high as 80 Ra with an increase of 59.3 Vol% b4c particle.

Poovazhagan et al. [25] studied the added Nanob4c in AMCs and enhanced its hardness, tensile strength, wear resistance, and good ductility, and impact resistance of the Al alloy was retained.

Graphite is another important secondary reinforcement material because of its constructive dry sliding wear condition for AMCs. In the current research, graphite favoured in AMCs improved both wear resistance and machinability. The incorporation of graphite diminishes the surface porosity and enhances mechanical and tribological properties continuously [26–28].

Saini et al. [29] observed that hardness of the hybrid composite had increased significantly to added nanosilica particles and graphite flake as reinforcements. These new hybrid composites can be used for various applications including engine piston, automobile components, and microelectronic devices.

Zhang et al. [30] prepared two variety composites Al-Sic-graphite and Al-Sic-graphene and observed reinforcement and microstructure by using SEM, TEM, XRD, and Raman spectroscopy. The added graphite flake reinforcement is partly desquamated into thinner ones, and the clusters of graphite with a size as large as 10 μm can still be observed in the Al-graphite sample.

Alaneme et al. [31] developed Al-Mg-Si alloy with steel and graphite particle composites prepared by stir casting. All the mechanical properties are reduced slightly with an augment in graphite content and trailed the composite reinforced with 8 wt.% steel.

Fe_3O_4 is a third reinforcement, and it plays an important role in the aerospace industry. The addition of Fe_3O_4 nanoparticle reinforcements in the AMCs enhanced the magnetic permeability of composites and thermal properties lacking mechanical degradation [32]. Fereiduni et al. [33] used Fe_3O_4 nanoparticles in the welding process to Al-Fe intermetallics due to their small size and heat generated.

AMCs produced with selective laser melting (SLM) have attracted all embracing attention in the lightweight application fields [34]. AMCs manufactured by SLM efficiently can accomplish greater mechanical properties compared to conventional manufacturing. Martin et al. [35] reported crack-free AA7075 elements achieved by mixing nano-ZrH_2 particles with 7075 powder before SLM. All through solidification, the recently shaped Al_3Zr phase obviously assisted granule modification, because of which the mechanical properties are enhanced. Gu et al. [36] discussed that the effect of nanoparticle reinforcement on the strength and ductility of materials is enhanced simultaneously as manufactured by SLM. Zhang et al. [37] fabricated SiC/$AlSi_{10}Mg$ composites by SLM technique, and the microstructure and mechanical properties of composites are investigated. The AMCs show the highest yield strength and modulus among values of 408 MPa and 90 GPa, respectively. In the current research work, the AMCs-B_4C-Gr-Fe_3O_4 hybrid composite is fabricated by selective laser melting (SLM) and investigated tensile, hardness, and microstructure.

2. Experimental Details

2.1. Powder Preparation. The experiment's matrix materials were A356 alloy powder (60 m, =2.662 g/cc) acquired from Bhoomi Metal & Alloys in Maharashtra. B_4C powder (30 m, 2.25 g/cc), Gr powder (100 m, 2.26 g/cc), and Fe_3O_4 powder (60 m, 4.9 g/cc) were acquired from Intelligent Materials Private Limited in Punjab and Saveer Biotech Limited in Uttar Pradesh, respectively. In a planetary ball mill, three samples (2, 4, and 6) of the A356-B_4C-Gr-Fe_3O_4 hybrid composite powder were prepared. The details of the sample powder are mentioned in Table 1.

2.2. SLM Process. The A356-B_4C-Gr-FE_3O_4 specimens were created on an SLM machine designed by ARCI in Hyderabad, India, as shown in Figure 1. An SLM machine is fitted with a fiber laser with a wavelength of 1076 nm. The entire experiment was carried out with a continuous-wave laser with a power of 400 W and a spot size of 110 m. To prevent the specimens from oxidising, the SLM procedure was carried out in a vacuum, as described in earlier literature reviews [25–27]. The pressure in the chamber was fixed at 6×10^{-3} Pa. In addition, an argon gas flow was incorporated into the experimental setting in order to evaluate the impact of atmospheric conditions on the make superiority. The chamber was emptied to the abovementioned pressure. During laser irradiation, the chamber pressure was adjusted to $1.5 \cdot 10^3$ Pa by using argon gas to produce flow. Table 2 and

Table 1: Sample powder details.

Sample no.	Composite powder	A356	B_4C	Gr	FE_3O_4
1		94	2	2	2
2	A356-B_4C-Gr-FE_3O_4	88	4	4	4
3		82	6	6	6

Figure 1: The SLM experimental setup.

Table 2: The list of SLM process machine specifications and laser process parameters.

Fiber laser	400 W
Spot sizes	80-115 μm
Scan processing speed	10 m/s
Build area	280 × 280 × 365 mm
Layer thickness	20-100 μm
Platform heating	200°C

Figure 2 show the process parameters and SLM procedure. The experiment was carried out with each combination of process parameters to construct single-layer samples with a dimension of 14 mm × 100 mm.

3. Testing of Composite

3.1. Microstructural Investigation. The optical microscope was used to examine the SLM specimens, as illustrated in Figure 3. To produce a better disparity, the samples were ground with 220, 400, 600, and 1000 grades of emery paper, then refined with diamond suspensions of 6, 4, and 2 mm diameters, and etched using Kroll's reagent (15 mL of HF, 40 mL of HNO_3, and 60 mL of water, ASTM E407) for 30 seconds. Optical microscopy was used to investigate the microstructure (1000x magnifications, GX51, Olympus).

3.2. Microhardness. When test samples are very small or thin in a composite sample, microhardness testing is a technique for estimating a material's hardness on a microscopic scale. Microhardness was assessed on this specimen using UHL VMHT digital microhardness equipment, as illustrated in Figure 4. Ranges of indents may be completed on the sample with the aid of computer control, and the hardness can be computed (load range from 0.3 to 30 kgf) for the purpose of detachment from an orientation point. This microhardness apparatus is very well suited to create fractures on the sample surface, allowing the rupture robustness to be assessed.

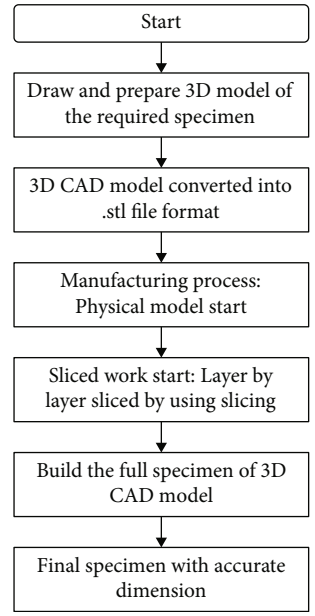

Figure 2: Flow chart of SLM process.

Figure 3: Optical microscope.

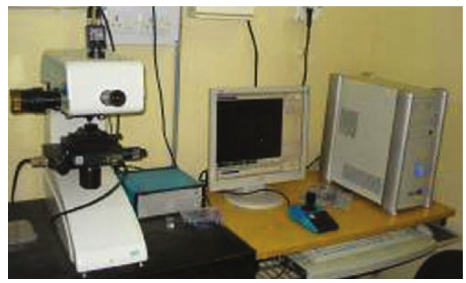

Figure 4: Microhardness tester (UHL VMHT digital).

3.3. Tensile Test. Microtension tests are used to measure the strength and ductility of nanocomposites under uniaxial tensile stresses in the development of novel alloys for quality control, commercial shipment acceptance testing, and structural design assistance. It was validated in accordance

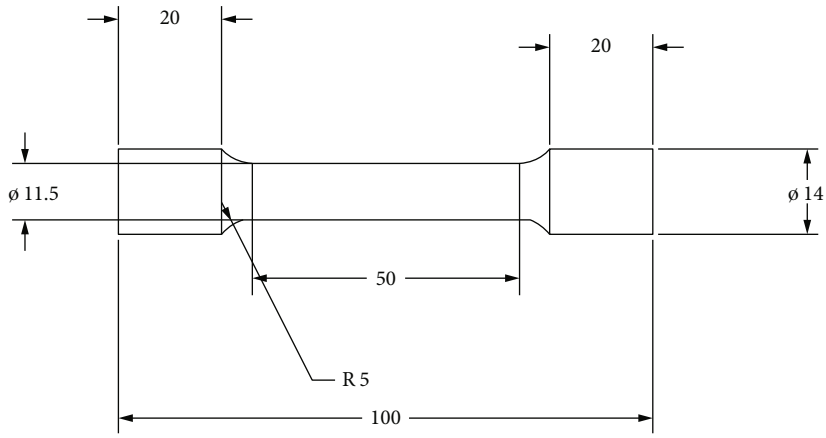

Figure 5: Microtensile test specimen.

Figure 6: Multipurpose microtensile testing machine.

Figure 7: Scanning electron microscopy (SEM).

with ASTM B-557M standards using three specimens, each measuring 100 mm in length and 14 mm in diameter, as illustrated in Figure 5 for each AMC family. The microtension was customary in any form at room temperature specifically the methods of determination of yield strength, yield point, elongation, tensile strength, and reduction of area. The multipurpose microtensile testing machine type (Max. static load ± 3000 N and Max. dynamic load ± 2500 N) among dutiful seize is used to hold the tensile specimen as shown in Figure 6.

3.4. SEM. In the microanalysis and failure analysis of nanocomposites, scanning electron microscopy (SEM) is used very professionally. It is done at high exaggerations, produces high-resolution pictures, and precisely measures very small facial features and objects. By rastering a focused electron beam across the surface and distinguishing between generated and backscattered electron signals, SEM offers comprehensive high-resolution images of the material. Figure 7 shows the SEM.

4. Result and Discussion

4.1. Microstructure. Figure 8 shows the fascia microstructures of A356 with 2, 4, and 6% B4C-Gr-Fe_3O_4 at magnifications of 100. The nanocomposite specimen remained sophisticated in terms of removing particles from the surface. Optical microscopes are expected to support particle distribution vestiges. The additive manufacturing process was inspected under an optical microscope to determine the specimen reinforcement pattern. The homogeneous dispersion of nanoparticles in the matrix material of the A356 alloy was clearly visible. The presence of nanoparticles leads to the formation of cracks, which leads to elastic deformation with increases in load. Composite rupture is represented by dimples, voids, clusters, and cracks. Fragile composite fracture in the form of cracks and rupture is due to the strong interfacial bonding between the reinforcements and the A356 matrix.

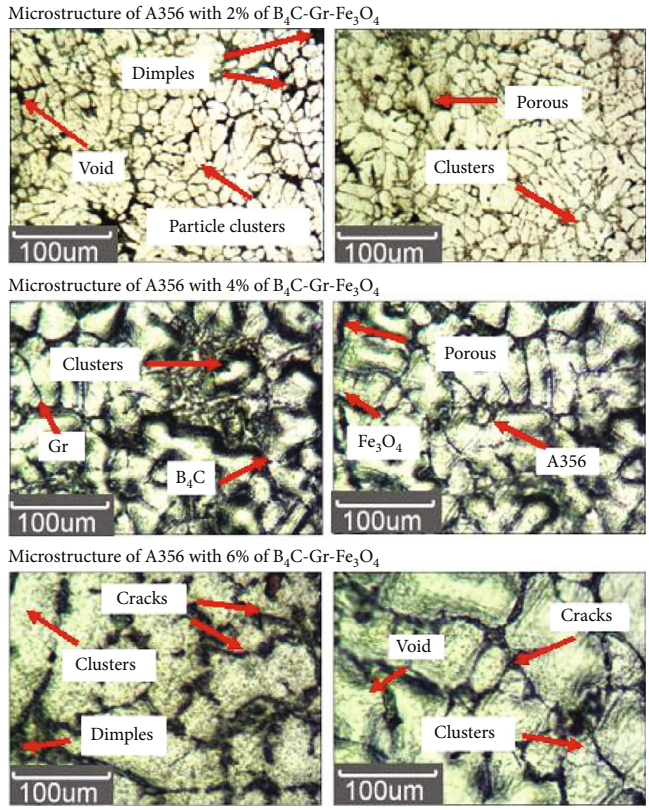

Figure 8: Microstructure of A356 with reinforcement B_4C-Gr-Fe_3O_4.

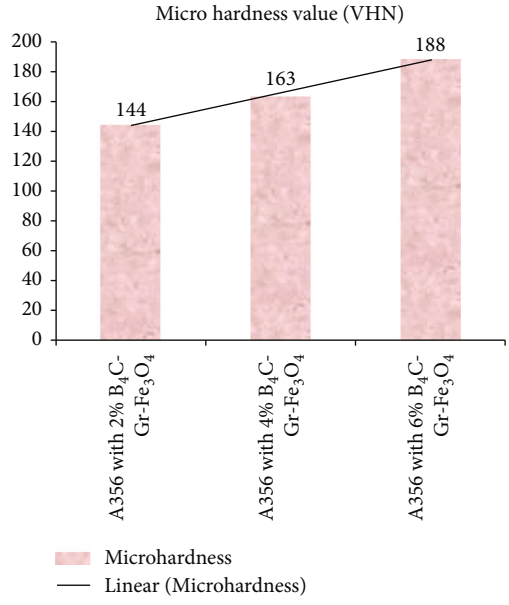

Figure 9: The microhardness values.

4.2. Microhardness. The specimen for the microhardness test was prearranged with a length and diameter of 10 mm × 12 mm. The surface to be examined should have a metallographic finish; hence, emery sheets of various grit sizes (100-1000) were used to finish the surface.

Table 3: Microhardness value of A356 with B_4C-Gr-Fe_3O_4 hybrid composites.

	Microhardness value (VHN)
A356 with 2% B_4C-Gr-Fe_3O_4	144
A356 with 4% B_4C-Gr-Fe_3O_4	163
A356 with 6% B_4C-Gr-Fe_3O_4	188

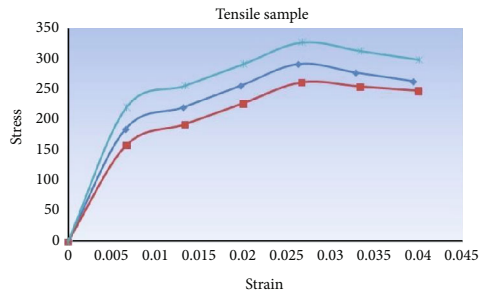

Figure 10: Stress vs. strain (UTS value in N/mm^2).

Table 4: Ultimate strength value of A356 with B_4C-Gr-Fe_3O_4 hybrid composites.

	Ultimate strength value (N/mm^2)
A356 with 2% B_4C-Gr-Fe_3O_4	260.10
A356 with 4% B_4C-Gr-Fe_3O_4	290.06
A356 with 6% B_4C-Gr-Fe_3O_4	325.43

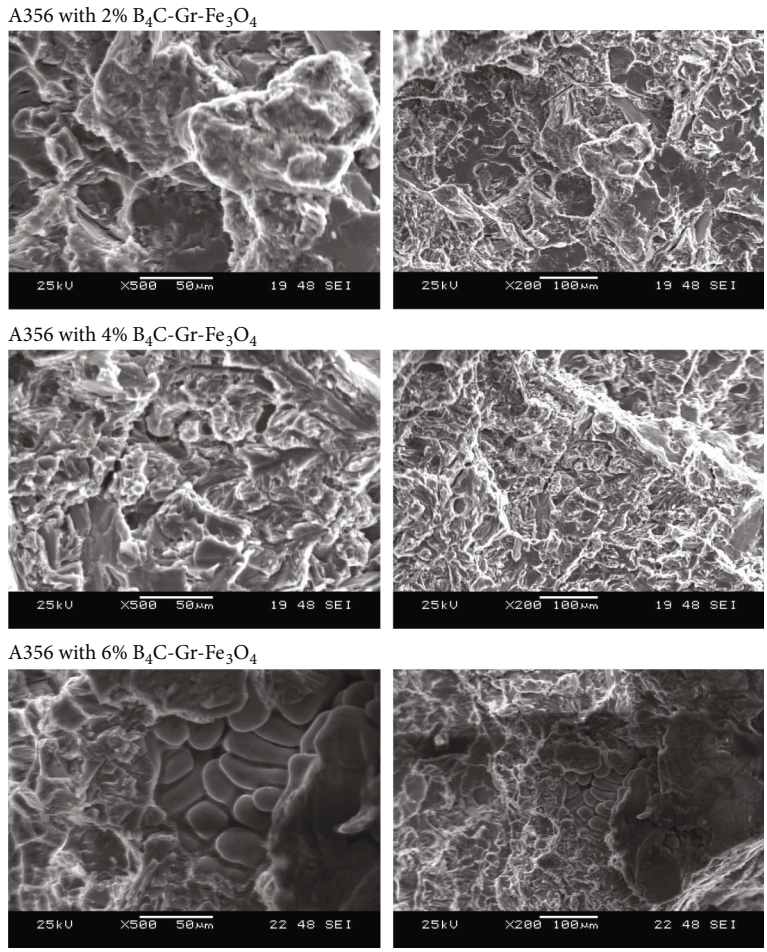

Figure 11: FESEM of tensile specimen (fracture analysis).

Equation (1) calculates the microhardness:

$$\mathrm{MH} = \frac{\mathrm{MAL}}{\mathrm{AI}}, \tag{1}$$

where,

MH is microhardness

MAL is maximum applied load, and

AI is the area of indentation.

The Vickers Hardness Number (VHN) for A356 with 2, 4, and 6% reinforcement is 144, 163, and 188, respectively. With the reinforcement of 4% graphite and 3% ferrous oxide, the microhardness value of LM25 was 112. As the percentage of graphite (Gr) in the composites increases, the hardness of the normal particles falls [38]. When compared to matrix A356 alloy, the combined BHN value of A356/Gr/B_4C is 63.1 and the hardness value of the hybrid composite increased by roughly 56.1 percent. The harder B_4C ceramic particles are responsible for the increased hardness [39–41]. The research used A356 nanoparticles and reinforcements to achieve the better improvement in microhardness demonstrated in Figure 9 and Table 3.

4.3. Tensile Test. The ultimate tensile strength and stress-strain of the composites are improved with increased reinforcement, as shown in Figure 10. The variance in ultimate tensile strength with the AMMCs is shown in Table 4. The load value of graphite and iron oxide (2, 4, and 6 percent) increases as the boron carbide reinforcement is increased. 260.10, 290.06, and 325.43 $\mathrm{N/mm^2}$ are the maximum ultimate tensile strengths, respectively [40, 41].

4.4. FESEM. When the manufactured composite material was subjected to fracture analysis, the results were as indicated in Figure 11. The FESEM image of the broken surface shows the mixing behaviour of ductile fracture, brittle fracture, and ploughing of reinforced material. Ductile fracture behaviour is caused by plastic deformation of the material prior to fracture, which results in the creation of a hollow. The quick and sudden fracture under stress causes brittle fracture behaviour. Transverse ruptures cause the ploughing fracture, which results in a deep hole-like cavity. All of these point to the fracture mixing behaviour [41].

5. Conclusion

SLM successfully created hybrid nanocomposites of B_4C-GFe_3O_4 with varied reinforcements (2, 4, and 6). The microstructural analysis demonstrated that particles were distributed uniformly throughout the matrix material.

Fractographic analysis was used to examine the tensile characteristics of the produced MMCs. The following are the results and conclusions of the hardness and tensile test:

(i) The microhardness of nanocomposite A356 with 2, 4, and 6% reinforcement is 144, 163, and 188 VHN, according to the findings of a microhardness test

(ii) Tensile testing of nanocomposite A356 with 2, 4, and 6% reinforcement yielded 260.10, 290.06, and 325.43 N/mm^2, respectively

(iii) The fractographic images reveal a combination of ductile and brittle fracture behaviours, as well as ploughing of reinforced material

(iv) Ductile fracture behaviour is caused by plastic deformation of the material prior to fracture, which results in the creation of a hollow. The quick and sudden fracture under stress causes brittle fracture behaviour. Transverse ruptures cause the ploughing fracture, which results in a deep hole-like cavity

Data Availability

The data used to support the findings of this study are included in the article. Should further data or information be required, these are available from the corresponding author and upon request.

Conflicts of Interest

The authors declare that they have no conflicts of interest.

References

[1] S. Dadbakhsh, R. Mertens, L. Hao, J. Van Humbeeck, and J.-P. Kruth, "Selective laser melting to manufacture "in situ" metal matrix composites: a review," *Advanced Engineering Materials*, vol. 21, no. 3, article 1801244, 2019.

[2] T. B. Sercombe and X. Li, "Selective laser melting of aluminium and aluminium metal matrix composites: review," *Materials Technology*, vol. 1–9, 2015.

[3] B. Jiang, L. Zhenglong, C. Xi, L. Peng, L. Nannan, and C. Yanbin, "Microstructure and mechanical properties of TiB_2-reinforced 7075 aluminum matrix composites fabricated by laser melting deposition," *Ceramics International*, vol. 45, no. 5, pp. 5680–5692, 2019.

[4] N. Verma and S. C. Vettivel, "Characterization and experimental analysis of boron carbide and rice husk ash reinforced AA7075 aluminium alloy hybrid composite," *Journal of Alloys and Compounds*, vol. 741, pp. 981–998, 2018.

[5] D. Bandhu, A. Thakur, R. Purohit, R. K. Verma, and K. Abhishek, "Characterization & evaluation of Al_{7075} MMCs reinforced with ceramic particulates and influence of age hardening on their tensile behavior," *Journal of Mechanical Science and Technology*, vol. 32, no. 7, pp. 3123–3128, 2018.

[6] M. Ravichandran, A. Naveen Sait, and V. Anandakrishnan, "Al–TiO_2–Gr powder metallurgy hybrid composites with cold upset forging," *Rare Metals*, vol. 36, pp. 686–696, 2014.

[7] H. S. Kumaraswamy, V. Bharath, and T. Krishna Rao, "Microstructure and mechanical properties of sintered Al_{2024} hybrid MMCs," *Journal of Physics: Conference Series*, vol. 1455, no. 1, article 012024, 2020.

[8] A. Alizadeh, M. Maleki, and A. Abdollahi, "Preparation of super-high strength nanostructured B_4C reinforced Al-2Cu aluminum alloy matrix composites by mechanical milling and hot press method: microstructural, mechanical and tribological characterization," *Advanced Powder Technology*, vol. 28, no. 12, pp. 3274–3287, 2017.

[9] J. Mohamadigangaraj, S. Nourouzi, and H. Jamshidi Aval, "The effect of heat treatment and cooling conditions on friction stir processing of A390-10 wt% SiC aluminium matrix composite," *Materials Chemistry and Physics*, vol. 263, article 124423, 2021.

[10] M. M. Moradi, H. J. Aval, and R. Jamaati, "Effect of pre and post welding heat treatment in SiC-fortified dissimilar AA6061-AA2024 FSW butt joint," *Journal of Manufacturing Processes*, vol. 30, pp. 97–105, 2017.

[11] A. Mohamed and F. Samuel, "A review on the heat treatment of Al-Si-Cu/Mg casting alloys," *Heat Treatment-Conventional and Novel Applications*, vol. 1, pp. 55–72, 2012.

[12] V. Suresh, N. Hariharan, and S. Vellingiri, "An investigation on the tensile properties and micro-structure of hybrid metal matrix composites," *International Journal of Materials and Product Technology*, vol. 56, no. 1/2, pp. 84–94, 2018.

[13] M. Jawaid and M. Thariq, *Handbook Sustainable Composites for Aerospace Applications*, Woodhead Publishing, Cambridge, 2018.

[14] J. Anoop and S. Vijay Ananth, "Fabrication process and characterization of A356 aluminium alloy reinforced with Gr-FE_3O_4-B_4C hybrid nanoparticles manufactured by selective laser melting (SLM)," in *4th International Conference on Advances in Mechanical Engineering*, p. 238, Chennai, 2022.

[15] N. K. Bhoi, H. Singh, and S. Pratap, "Developments in the aluminum metal matrix composites reinforced by micro/nano particles – a review," *Journal of Composite Materials*, vol. 54, no. 6, pp. 813–833, 2020.

[16] S. Saravanan, A. Godwin Antony, V. Vijayan, M. Loganathan, and S. Baskar, "Synthesis of SiO_2 nano particles by using sol-gel route," *International Journal of Mechanical Engineering and Technology*, vol. 1, pp. 785–790, 2019.

[17] M. Cabeza, I. Feijoo, P. Merino et al., "Effect of high energy ball milling on the morphology, microstructure and properties of nano-sized TiC particle-reinforced 6005A aluminium alloy matrix composite," *Powder Technology*, vol. 321, pp. 31–43, 2017.

[18] S. J. S. Chelladurai, R. Arthanari, K. Krishnamoorthy, K. S. Selvaraj, and P. Govindan, "Effect of copper coating and reinforcement orientation on mechanical properties of LM6 aluminium alloy composites reinforced with steel mesh by squeeze casting," *Transactions of the Indian Institute of Metals*, vol. 71, no. 5, pp. 1041–1048, 2018.

[19] M. Senthil Kumar, M. Vanmathi, and G. Sakthivel, "SiC reinforcement in the synthesis and characterization of A356/Al_2O_3/SiC/Gr reinforced composite-paving a way for the next generation of aircraft applications," *Silicon*, vol. 13, no. 8, pp. 2737–2744, 2021.

[20] S. Das, M. Chandrasekaran, S. Samanta, P. Kayaroganam, and P. Davim, "Fabrication and tribological study of AA6061 hybrid metal matrix composites reinforced with SiC/B_4C nanoparticles," *Industrial Lubrication and Tribology*, vol. 71, no. 1, pp. 83–93, 2019.

[21] M. J. Nasr Isfahani, F. Payami, M. A. Asadabad, and A. A. Shokri, "Investigation of the effect of boron carbide nanoparticles on the structural, electrical and mechanical properties of Al-B_4C nanocomposites," *Journal of Alloys and Compounds*, vol. 797, pp. 1348–1358, 2019.

[22] L. Poovazhgan, S. Vijayananth, and S. Sivaganesan, "Optimizing ultrasonic power on fabricating aluminum nanocomposites reinforced with boron carbide nanoparticles," *Materials Science Forum*, vol. 979, pp. 28–33, 2020.

[23] G. Dirisenapu, L. Dumpala, and S. P. Reddy, "The influence of B_4C and BN nanoparticles on Al 7010 hybrid metal matrix nanocomposites," *Emerging Materials Research*, vol. 9, no. 3, pp. 558–563, 2020.

[24] S. Chandrasekaran, R. Lu, R. Landingham et al., "Additive manufacturing of graded B_4C-Al cermets with complex shapes," *Materials & Design*, vol. 188, article 108516, 2020.

[25] L. Poovazhagan, K. Kalaichelvan, and T. Sornakumar, "Processing and performance characteristics of aluminum-nano boron carbide metal matrix nanocomposites," *Materials and Manufacturing Processes*, vol. 31, no. 10, pp. 1275–1285, 2016.

[26] S. Arif, B. Jamil, M. B. N. Shaikh, T. Aziz, A. H. Ansari, and M. Khan, "Characterization of surface morphology, wear performance and modelling of graphite reinforced aluminium hybrid composites," *Engineering Science and Technology, an International Journal*, vol. 23, no. 3, pp. 674–690, 2019.

[27] B. Guntreddi and A. Ghosh, "Anti-frictional role of diamond and graphite suspended bio-oil based nano- aerosols at sliding interface of Al-SiC_p and WC-6Co," *Tribology International*, vol. 153, article 106596, 2021.

[28] S. Mohamad, S. Liza, and Y. Yaakob, "Strengthening of the mechanical and tribological properties of composite oxide film formed on aluminum alloy with the addition of graphite," *Surface and Coatings Technology*, vol. 403, article 126435, 2020.

[29] S. Saini, A. Gupta, A. J. Mehta, and S. Pramanik, "Rice husk-extracted silica reinforced graphite/aluminium matrix hybrid composite," *Journal of Thermal Analysis and Calorimetry*, vol. 147, pp. 1157–1166, 2022.

[30] J. Zhang, Q. Liu, S. Yang, Z. Chen, Q. Liu, and Z. Jiang, "Microstructural evolution of hybrid aluminum matrix composites reinforced with SiC nanoparticles and graphene/graphite prepared by powder metallurgy," *Progress in Natural Science: Materials International*, vol. 30, no. 2, pp. 192–199, 2020.

[31] K. K. Alaneme, A. V. Fajemisin, and N. B. Maledi, "Development of aluminium-based composites reinforced with steel and graphite particles: structural, mechanical and wear characterization," *Journal of Materials Research and Technology*, vol. 8, no. 1, pp. 670–682, 2019.

[32] N. Ashrafi, A. H. M. Ariff, M. Sarraf, S. Sulaiman, and T. S. Hong, "Microstructural, thermal, electrical, and magnetic properties of optimized Fe_3O_4-SiC hybrid nano filler reinforced aluminium matrix composite," *Materials Chemistry and Physics*, vol. 258, p. 123895, 2021.

[33] E. Fereiduni, M. Movahedi, and A. Baghdadchi, "Ultrahigh-strength friction stir spot welds of aluminium alloy obtained by Fe_3O_4 nanoparticles," *Science and Technology of Welding and Joining*, vol. 23, no. 1, pp. 63–70, 2017.

[34] M. P. Behera, T. Dougherty, and S. Singamneni, "Conventional and additive manufacturing with metal matrix composites: a perspective," *Procedia Manufacturing*, vol. 30, pp. 159–166, 2019.

[35] J. H. Martin, B. D. Yahata, J. M. Hundley, J. A. Mayer, T. A. Schaedler, and T. M. Polock, "3D printing of high-strength aluminium alloys," *Nature*, vol. 549, no. 7672, pp. 365–369, 2017.

[36] D. Gu, H. Wang, D. Dai, P. Yuan, W. Meiners, and R. Poprawe, "Rapid fabrication of Al-based bulk-form nanocomposites with novel reinforcement and enhanced performance by selective laser melting," *Scripta Materialia*, vol. 96, pp. 25–28, 2015.

[37] Y. Zhang, J. Sun, and R. Vilar, "Characterization of (TiB + TiC)/TC_4 in situ titanium matrix composites prepared by laser direct deposition," *Journal of Materials Processing Technology*, vol. 211, no. 4, pp. 597–601, 2011.

[38] P. Ravindran, K. Manisekar, P. Narayanasamy, N. Selvakumar, and R. Narayanasamy, "Application of factorial techniques to study the wear of Al hybrid composites with graphite addition," *Materials and Design*, vol. 39, pp. 42–54, 2012.

[39] P. R. Jadhav, B. R. Sridhar, M. Nagaral, and J. I. Harti, "Mechanical behavior and fractography of graphite and boron carbide particulates reinforced A356 alloy hybrid metal matrix composites," *Advanced Composites and Hybrid Materials*, vol. 3, no. 1, pp. 114–119, 2020.

[40] S. Vellingiri, "An experimental and investigation on the micro-structure hardness and tensile properties of Al-GrFe_3O_4 hybrid metal matrix composites," *FME Transactions*, vol. 47, no. 3, pp. 511–517, 2019.

[41] V. Suresh, P. Vikram, R. Palanivel, and R. F. Laubscher, "Mechanical and wear behavior of LM25 aluminium matrix hybrid composite reinforced with boron carbide, graphite and iron oxide," *Materials Today: Proceedings*, vol. 5, pp. 27852–27860, 2018.